Research Square

Preprints are preliminary reports that have not undergone peer review.
They should not be considered conclusive, used to inform clinical practice,
or referenced by the media as validated information.

# 1,25-Dihydroxyvitamin D3 Alleviates High Glucose-Induced Oxidative Stress and Rescues Osteogenic Differentiation of Human Periodontal Ligament Stem Cells via the NRF2/HO-1 Signaling Pathway

**Wenjie Yang**
Lanzhou University
**Qian Huang**
Lanzhou University
**Chupeng Huang**
Lanzhou University
**Siqi Li**
Lanzhou University
**Lulu Cai**
Lanzhou University
**Jingxuan Tu**
Lanzhou University
**Xinyue Zhang**
Lanzhou University
**Xiaoli An**
Lanzhou University
**Qingzong Si**
Siqz@lzu.edu.cn
Lanzhou University

**Research Article**

**Keywords:** High glucose, Human periodontal ligament stem cells, 1,25-Dihydroxyvitamin D3, Oxidative stress, Osteogenic differentiation

**Posted Date:** November 4th, 2026

**DOI:** https://doi.org/10.21203/rs.3.rs-11385599/v1

**License:** This work is licensed under a Creative Commons Attribution 4.0 International License.
Read Full License

**Additional Declarations:** No competing interests reported.

# Title Page

**[Article Type]:** Original Research Article

**[Article Title]:**

***1,25-Dihydroxyvitamin $D_3$ Alleviates High Glucose-Induced Oxidative Stress and Rescues Osteogenic Differentiation of Human Periodontal Ligament Stem Cells via the NRF2/HO-1 Signaling Pathway***

**[Author List]:**

Wenjie Yang[a,b], Qian Huang[a,b], Chupeng Huang[a,b], Siqi Li[a,b], Lulu Cai[a,b], Jingxuan Tu[a,b], Xinyue Zhang[a,b], Xiaoli An[a,b,*] and Qingzong Si[a,b,*]

[a] Key Laboratory of Dental Maxillofacial Reconstruction and Biological Intelligence Manufacturing, School/Hospital of Stomatology, Lanzhou University, Lanzhou 730000, Gansu Province, PR China

[b] School/Hospital of Stomatology, Lanzhou University, Lanzhou, Gansu Province, PR China.

Wenjie Yang: Email: ywj0137@163.com

Qian Huang: Email: qianhuang0630x@163.com

Chupeng Huang: Email: 2405632353@qq.com

Siqi Li: Email: lisiqi2025@lzu.edu.cn

Lulu Cai: Email: caill2025@lzu.edu.cn

Jingxuan Tu: Email: tjx15544930716@163.com

Xinyue Zhang: Email: zxy247986@qq.com

* Corresponding Authors:

Primary Corresponding Author: Qingzong Si, Email: Siqz@lzu.edu.cn

Co-Corresponding Author: Xiaoli An, Email: Anxl@lzu.edu.cn

These authors contributed equally to this work.

**[Statements]:**

**1. Data availability statement**

All data generated or analysed during this study are included in this published article.

**2. Funding statement**

This work was supported by the Natural Science Foundation of Gansu Province (26JRRA197) and the Joint Research Fund of Gansu Province (26JRRA963 and 26JRRA962).

**3. Conflict of interest disclosure**

We declare that we have no known competing financial interests or personal relationships that could have appeared to influence the work reported in this paper.

**4. Ethics approval statement**

All procedures performed in this study adhered to the tenets of the Declaration of Helsinki and were approved by the Ethics Committee of the School of Stomatology, Lanzhou University (No. LZUKQ-2025-073), following the obtainment of informed consent from all participants.

**5. Patient consent statement**

Written informed consent was obtained from all individual participants included in the study, including consent for the publication of their data.

**Abstract**

Periodontitis is a chronic infectious disease caused by dental plaque biofilms, driving progressive destruction of periodontal supporting tissues. Diabetes mellitus is recognized as a major risk factor for this disease. Hyperglycemia-induced oxidative stress severely impairs the osteogenic differentiation of human periodontal ligament stem cells (hPDLSCs), thereby hindering periodontal bone regeneration. 1,25-Dihydroxyvitamin $D_3$ [$1,25(OH)_2D_3$] has been confirmed to possess both antioxidant and pro-osteogenic activities; however, its specific regulatory effects on hPDLSCs under high-glucose conditions remain poorly elucidated. This study aimed to construct a high glucose-induced oxidative stress injury model in hPDLSCs to investigate the effects of $1,25(OH)_2D_3$ on oxidative stress and osteogenic differentiation, and to elucidate the underlying molecular mechanisms, so as to provide a theoretical basis and identify novel therapeutic targets for periodontal bone regeneration in diabetes-associated periodontitis. Our results demonstrated that high glucose exposure inhibited the proliferation, migration and osteogenesis of hPDLSCs, while concurrently increasing oxidative stress and inflammatory responses. $1,25(OH)_2D_3$ alleviates high glucose-induced oxidative stress damage and rescues the impaired osteogenic differentiation of hPDLSCs via activating the NRF2/HO-1 signaling pathway. Collectively, these findings indicate that $1,25(OH)_2D_3$ represents a promising therapeutic candidate for periodontal bone regeneration in patients with diabetic periodontitis.

Keywords: High glucose; Human periodontal ligament stem cells; 1,25-Dihydroxyvitamin $D_3$; Oxidative stress; Osteogenic differentiation

## 1. Introduction

Periodontitis is a chronic inflammatory disease primarily initiated by bacterial biofilms, and diabetes mellitus is widely recognized as a major risk factor that exacerbates its progression (Kwon et al. 2021; Păunică et al. 2023; Preshaw et al. 2012). In patients with diabetic periodontitis, sustained high glucose disrupts local metabolic homeostasis and induces severe oxidative stress through the excessive generation of reactive oxygen species (Ceriello and Prattichizzo 2021; Zhang et al. 2023). This persistent oxidative

microenvironment directly damages periodontal tissues, amplifies local inflammation via advanced glycation end-products, and severely impairs the function of osteoblasts, leading to exacerbated alveolar bone loss (Meng and Wen 2025; Plemmenos and Piperi 2022; Xiang et al. 2025; Cheng et al. 2022; Norahan et al. 2025). Traditional mechanical debridement and guided tissue regeneration therapies often fail to achieve predictable bone reconstruction in diabetic patients, as these physical and barrier-based interventions cannot reverse the underlying high glucose-driven metabolic dysfunction and severe oxidative damage (Hajishengallis et al. 2020; Zheng et al. 2026). Therefore, there is an urgent clinical need to explore targeted strategies that actively mitigate high glucose-induced oxidative stress to restart the regenerative program in periodontal bone tissues (He et al. 2022; Tian et al. 2025; Chen et al. 2025).

Human periodontal ligament stem cells (hPDLSCs) are multipotent mesenchymal stem cells that serve as the primary cellular basis for periodontal tissue regeneration (Romain et al. 2025; Chen et al. 2025). Under physiological conditions, hPDLSCs exhibit robust osteogenic differentiation and immunomodulatory capacities (Zakaria et al. 2024; Alves et al. 2026). However, in an high glucose-mediated metabolic microenvironment, their biological functions are severely compromised (Zhang et al. 2022). Intracellular reactive oxygen species (ROS) accumulation disrupts redox homeostasis, inducing lipid peroxidation and suppressing critical osteogenic signaling pathways (Mateen et al. 2024; Wada et al. 2026; Meng et al. 2022; Cao et al. 2025). Consequently, the expression of essential osteogenic regulators at both the transcriptional and translational levels is significantly downregulated, ultimately depriving hPDLSCs of their regenerative potential (Wang et al. 2023; Song et al. 2025). Reversing this specific metabolic toxicity and restoring the osteogenic capacity of hPDLSCs remains a central challenge in diabetic periodontal therapy.

1,25-Dihydroxyvitamin $D_3$ [1,25$(OH)_2D_3$], the active metabolite of vitamin $D_3$, plays a pivotal role in regulating calcium-phosphorus metabolism and bone remodeling (Goltzman 2018; van Driel and van Leeuwen 2023). Beyond its classical skeletal functions, 1,25$(OH)_2D_3$ exhibits potent immunomodulatory and antioxidant properties (Palacios and Gonzalez 2014; Borojević et al. 2022). Recent studies have demonstrated that 1,25$(OH)_2D_3$ can alleviate oxidative stress and maintain cellular redox homeostasis, primarily by activating the nuclear factor erythroid 2-related factor 2 signaling pathway and its downstream antioxidant enzymes, such as heme oxygenase-1 (Li et al. 2023; Yang et al. 2022; Yuan et al. 2024). Moreover, 1,25$(OH)_2D_3$ has been shown to rescue

the osteogenic differentiation of hPDLSCs compromised by bacterial lipopolysaccharide-induced inflammation (Blufstein et al. 2021; Gong et al. 2022). Despite its proven efficacy in bacterial infection models, the specific effects of $1,25(OH)_2D_3$ on hPDLSCs within a high glucose -induced metabolic stress microenvironment remain largely unknown. It is yet to be elucidated whether $1,25(OH)_2D_3$ can confer dual protection—antioxidant and osteo-promotive—to counteract the specific metabolic toxicity of prolonged hyperglycemia.

To address this gap and isolate the metabolic toxicity of diabetes mellitus from bacterial interference, this study established an high glucose-induced oxidative stress model in hPDLSCs. We aimed to investigate the regulatory effects of $1,25(OH)_2D_3$ on high glucose-induced oxidative stress and osteogenic differentiation, and to elucidate whether these protective mechanisms are dependent on the activation of the NRF2/HO-1 signaling pathway. Our findings will provide a critical theoretical foundation and novel therapeutic targets for the clinical application of $1,25(OH)_2D_3$ as an adjunctive regenerative intervention for periodontal bone defects in diabetic patients.

## 2. Materials and Methods

### 2.1 Isolation, Culture, and Identification of hPDLSCs

Human periodontal ligament stem cells (hPDLSCs) were isolated from healthy premolars or third molars (donors aged 13 – 20) with ethics approval (School of Stomatology, Lanzhou University, No. LZUKQ-2025-073) and informed written consent. Tissues were collagenase-digested, and cells were cultured in 20% FBS medium. Passages 3 – 5 were used. Mesenchymal phenotype and multilineage (osteogenic/ adipogenic) potential were verified via immunofluorescence, flow cytometry, and Alizarin Red S/Oil Red O staining.

### 2.2 Cell Viability Assay

The proliferation of P3 – P5 hPDLSCs ($7 \times 10^3$ cells/well) was evaluated using the CCK-8 assay. To determine optimal doses, cells were initially treated with $1,25(OH)_2D_3$ (1 – 300 nM) or high glucose (HG, 15 – 50 mM). Controls included 5.5 mM glucose (normal) and 5.5 mM glucose + 19.5 mM mannitol (osmotic control). Based on these screening results, 25 mM HG was selected as the optimal concentration for inducing cellular impairment, and 1, 10, and 100 nM of $1,25(OH)_2D_3$ were identified as the optimal protective gradients (Zhen et al. 2017; Liu et al. 2023). Subsequently, cells were co-treated with 25 mM HG and these optimal $1,25(OH)_2D_3$ gradients. CCK-

8 absorbance was measured at 450 nm at 12, 24, 48, and 72 h.

### 2.3 Scratch Wound Healing Assay

The migration capacity of hPDLSCs was assessed by scratch wound-healing assay. Cells ($5 \times 10^5$/well) in 6-well plates were grown to confluence, scratched with a 200 μL pipette tip, washed with PBS, and treated with four conditions based on optimal doses: Control (5.5 mM glucose), $1,25(OH)_2D_3$ (100 nM), HG (25 mM), and HG + $1,25(OH)_2D_3$ (25 mM + 100 nM). Wound images were taken at 0, 6, 12, and 24 h, and closure rates were quantified using ImageJ.

### 2.4 Measurement of Intracellular Reactive Oxygen Species

Intracellular ROS levels were evaluated using the DCFH-DA fluorescent probe. Briefly, treated hPDLSCs were incubated with 1:2000 DCFH-DA for 20 min at 37°C in the dark. For quantitative analysis, mean fluorescence intensity was immediately measured via flow cytometry after harvesting. For qualitative assessment, fluorescent signals of stained cells were visualized under an inverted fluorescence microscope.

### 2.5 Measurement of Lipid Peroxidation

Intracellular lipid peroxidation was evaluated by quantifying malondialdehyde (MDA) levels using a thiobarbituric acid (TBA) assay kit. After designated treatments, hPDLSCs were lysed and centrifuged. The supernatants were reacted with TBA solution at 100℃ for 15 min. Absorbance was measured at 532 nm, and final MDA concentrations were calculated using a standard curve, normalized to total protein content (BCA assay).

### 2.6 Measurement of Superoxide Dismutase (SOD) Activity

Intracellular SOD activity was evaluated using a WST-8 assay kit. After designated treatments, hPDLSCs were lysed and centrifuged. Supernatants were incubated with WST-8 solution at 37℃ for 30 min. Absorbance was measured at 450 nm, and SOD activity (U/mg protein) was calculated, normalized to total protein content (BCA assay).

### 2.7 Alkaline Phosphatase Staining and Activity Assay

To evaluate early osteogenesis, hPDLSCs were cultured in osteogenic induction medium for 7 days under four groups: Control, $1,25(OH)_2D_3$ (100 nM), HG (25 mM), and HG + $1,25(OH)_2D_3$. The NRF2 inhibitor ML385 (5 μM) was added for mechanistic studies (Liu et al. 2023; Hu et al. 2025). ALP expression was assessed via BCIP/NBT staining, and quantitative ALP activity (U/gprot) was measured at 520 nm, normalized to total protein content (BCA assay).

### 2.8 Alizarin Red S Staining and Mineralization Quantification

To evaluate late-stage osteogenesis, hPDLSCs were cultured in osteogenic induction medium for 21 days under identical groupings as the ALP assay. Calcium nodules were fixed and stained with 1% Alizarin Red S. Mineralization was qualitatively photographed via inverted microscopy, and quantitatively assessed by measuring the absorbance of the eluted dye at 560 nm against a standard curve.

**2.9 Real-Time Quantitative Polymerase Chain Reaction**

Total RNA from treated hPDLSCs was extracted and reverse-transcribed into cDNA. Quantitative real-time PCR was performed using a Q3 System. After 7 days of osteogenic induction (with or without the NRF2 inhibitor ML385), the relative mRNA expressions of inflammatory (*TNF*-α, *IL-6*), antioxidant (*NRF2*, *HO-1*), and osteogenic (*ALP*, *RUNX2*, *OCN*, β-*catenin*) markers were evaluated. Target genes were normalized to GAPDH (primers in Table 1) and calculated using the $2^{-\Delta\Delta Ct}$ method.

**2.10 Western Blot Analysis**

Total proteins were extracted using RIPA buffer and quantified via BCA assay. Equivalent proteins were separated by SDS-PAGE, transferred to membranes, and probed with primary antibodies against oxidative (NRF2, HO-1) and osteogenic (ALP, RUNX2, OCN, β-catenin) markers. Mechanistic verification included treatment with the NRF2 inhibitor ML385. Bands were visualized using ECL and quantified via densitometric analysis, normalized to GAPDH.

**2.11 Immunofluorescence Staining**

To evaluate protein expression and subcellular localization, treated hPDLSCs in confocal dishes were fixed, permeabilized, and blocked. Cells were incubated overnight at 4°C with primary antibodies against NRF2, HO-1, 8-OHdG, ALP, or RUNX2 (with or without the NRF2 inhibitor ML385 during 7-day osteogenesis). After incubation with fluorophore-conjugated secondary antibodies, cells were counterstained with phalloidin and DAPI. Fluorescence images were captured using a confocal laser scanning microscope.

**2.12 Enzyme-Linked Immunosorbent Assay(ELISA)**

The secretion of pro-inflammatory cytokines (TNF-α and IL-6) in the culture medium of treated hPDLSCs was quantified using ELISA kits. Briefly, cell-free supernatants were collected. Absorbance was measured at 450 nm, and final cytokine concentrations were calculated based on standard curves.

**2.13 Statistical analysis**

All experiments were independently repeated in triplicate. Statistical analysis was

performed using SPSS software. Quantitative data were expressed as mean ± standard deviation (Mean ± SD). The Shapiro – Wilk test and Levene's test were used to evaluate normality and homogeneity of variances, respectively. Since comparisons were focused on intergroup differences at individual time points rather than temporal trends, one way ANOVA was applied separately for each time point. Tukey's post hoc test was adopted for multiple comparisons when the variance was homogeneous; otherwise, the Games–Howell test was used. A two-tailed $P < 0.05$ was defined as statistically significant.

## 3. Results

### 3.1 Isolation, Culture, and Identification of hPDLSCs

Primary cells successfully migrated from tissue explants within one week, showing heterogeneous shapes initially and establishing a uniform fibroblast-like morphology with whorl-like patterns upon passaging (Fig. 1a,b). Immunofluorescence showed strong positivity for vimentin and negativity for cytokeratin, confirming their mesenchymal origin without epithelial contamination (Fig. 1e-h). Flow cytometry validated their MSC phenotype, with high expression of CD90, CD105, and STRO-1, but negligible CD34 and CD45 (Fig. 1i). Furthermore, Alizarin Red S and Oil Red O staining confirmed their osteogenic and adipogenic differentiation potential (Fig. 1c,d), verifying typical hPDLSC characteristics.

### 3.2 Effects of $1,25(OH)_2D_3$ on hPDLSCs Proliferation Under High Glucose Conditions

CCK-8 assays determined optimal intervention parameters. Low doses of $1,25(OH)_2D_3$ (1, 10 nM) promoted hPDLSC proliferation at 12 h, while high doses (200, 300 nM) were cytotoxic at 48 – 72 h. 100 nM was identified as the highest safe dose (Fig. 2a). High glucose (HG, 25 mM) significantly impaired viability starting at 24 h (survival dropping to 70% at 48 h), whereas mannitol controls ruled out osmotic interference (Fig. 2b). In rescue experiments, co-treatment with $1,25(OH)_2D_3$ (1 – 100 nM) effectively reversed HG-induced suppression at 24 h, peaking at 100 nM ($P < 0.001$). However, prolonged exposure (72 h) to ≥ 10 nM paradoxically exacerbated this suppression (Fig. 2c). Thus, 100 nM $1,25(OH)_2D_3$ against 25 mM HG for 24 h was selected for subsequent mechanistic studies.

### 3.3 Effects of $1,25(OH)_2D_3$ on hPDLSCs Migration Under High Glucose Conditions

An in vitro scratch wound-healing assay was performed to evaluate the effect of

$1,25(OH)_2D_3$ on the migration capacity of hPDLSCs under high glucose conditions. As shown in Fig. 2d, HG treatment significantly impaired cell migration, resulting in a delayed wound closure compared to the normal control at 6, 12, and 24 h. Conversely, co-treatment with $1,25(OH)_2D_3$ effectively attenuated this high glucose-induced impairment, significantly accelerating the wound closure rate and restoring the migratory capacity of hPDLSCs at both 12 and 24 h.

### 3.4 $1,25(OH)_2D_3$ Alleviates High Glucose-Induced Oxidative Stress in hPDLSCs

To evaluate redox homeostasis, we assessed ROS, MDA, and SOD levels. HG stimulation induced severe oxidative stress, evidenced by massive ROS accumulation, elevated lipid peroxidation (MDA), and impaired SOD activity. Co-treatment with $1,25(OH)_2D_3$ significantly reversed these damages: it suppressed ROS overproduction (Fig. 2e), mitigated MDA elevation (Fig. 2f), and restored SOD activity (Fig. 2g).

### 3.5 $1,25(OH)_2D_3$ Restores the Osteogenic Differentiation of hPDLSCs Impaired by High Glucose

To evaluate osteogenesis under HG conditions, we assessed early ALP activity (day 7) and late extracellular matrix mineralization (day 21). HG treatment significantly suppressed both ALP activity and calcium nodule formation, whereas $1,25(OH)_2D_3$ alone robustly enhanced their basal levels ($P < 0.001$). Importantly, co-treatment with $1,25(OH)_2D_3$ effectively attenuated HG-induced suppression, significantly restoring ALP staining/activity (Fig. 2h) and mineralized nodule deposition (Fig. 2i).

### 3.6 $1,25(OH)_2D_3$ Reverses High Glucose-Induced Downregulation of Osteogenic and Antioxidant Genes

To elucidate the molecular mechanisms, mRNA expressions of antioxidant, inflammatory, and osteogenic genes were evaluated. In the redox and inflammatory networks (Fig. 3a), HG significantly suppressed *NRF2* and *HO-1* transcription while upregulating *TNF*-α and *IL-6*. Conversely, co-treatment with $1,25(OH)_2D_3$ effectively reversed these aberrations, rescuing antioxidant defenses and suppressing inflammation. Regarding osteogenesis at day 7 (Fig. 4a), HG severely downregulated *ALP*, *RUNX2*, *OCN*, and β-*catenin*. $1,25(OH)_2D_3$ administration efficiently antagonized these deleterious effects, significantly restoring all evaluated osteogenic markers. $1,25(OH)_2D_3$ reshapes the transcriptional profile of hPDLSCs by enhancing antioxidant defense and reactivating osteogenesis under HG conditions.

### 3.7 $1,25(OH)_2D_3$ Restores the Expression of Antioxidant and Osteogenic Proteins Suppressed by High Glucose

Western blot confirmed these findings at the translational level. HG exposure significantly suppressed the protein levels of antioxidant (NRF2, HO-1; Fig. 3b) and osteogenic (ALP, RUNX2, OCN, β-catenin; Fig. 4b) markers. Conversely, co-administration of $1,25(OH)_2D_3$ effectively reversed HG-induced translational suppression, significantly restoring all evaluated antioxidant and osteogenic proteins. $1,25(OH)_2D_3$ mitigates HG metabolic toxicity by simultaneously rescuing endogenous antioxidant and osteogenic protein depletion.

### 3.8 $1,25(OH)_2D_3$ Suppresses the Secretion of Pro-inflammatory Cytokines Under High Glucose Conditions

ELISA quantified the immunomodulatory effects of $1,25(OH)_2D_3$. As shown in Fig. 3c, high glucose exposure drastically elevated TNF-α and IL-6 secretion, whereas $1,25(OH)_2D_3$ alone significantly suppressed their basal release. Importantly, co-treatment with $1,25(OH)_2D_3$ effectively antagonized the high glucose-induced inflammatory response, robustly reducing the secretion of both cytokines ($P < 0.001$).

### 3.9 $1,25(OH)_2D_3$ Rescues Expression and Localization of Antioxidant and Osteogenic Proteins

Immunofluorescence staining visualized target protein spatial distribution and expression. Basally, NRF2 and HO-1 showed low expressions, which $1,25(OH)_2D_3$ alone substantially intensified, notably driving NRF2 nuclear translocation. HG exposure severely diminished both signals, whereas co-treatment effectively reversed this downregulation and promoted NRF2 nuclear influx (Fig. 3e,f). Concurrently, HG-induced massive accumulation of the DNA damage marker 8-OHdG was significantly attenuated by $1,25(OH)_2D_3$ (Fig. 3d). Similarly, at day 7, co-treatment effectively antagonized HG-induced suppression of osteogenic markers, restoring robust extranuclear ALP and intense nuclear RUNX2 expressions (Fig. 4c,d).

### 3.10 $1,25(OH)_2D_3$ Promotes Osteogenic Differentiation via the NRF2/HO-1 Signaling Pathway

#### 3.10.1 $1,25(OH)_2D_3$ Activates the NRF2/HO-1 Pathway Under High Glucose Conditions

To verify NRF2/HO-1 pathway mediation, its activation was assessed via RT-qPCR, Western blot, and immunofluorescence. HG significantly suppressed NRF2 and HO-1 expression, which co-treatment with $1,25(OH)_2D_3$ effectively reversed, alongside promoting NRF2 nuclear translocation (Fig. 5a-d). Crucially, the NRF2 inhibitor ML385 completely abrogated all $1,25(OH)_2D_3$-induced transcriptomic/ translational

upregulations and blocked NRF2 nuclear accumulation, confirming targeted pathway dependency.

### 3.10.2 Inhibition of NRF2 Attenuates the Pro-osteogenic Effects of $1,25(OH)_2D_3$

We next investigated whether NRF2 blockade abolishes the osteogenic rescue effects of $1,25(OH)_2D_3$. Phenotypically, the addition of ML385 severely abrogated $1,25(OH)_2D_3$-restored ALP activity and mineralized nodule formation (Fig. 6a). Molecularly, the $1,25(OH)_2D_3$-induced upregulation of core osteogenic markers (ALP, RUNX2, OCN, β-catenin) was significantly reversed by ML385 at both mRNA and protein levels (Fig. 6b,c). Collectively, $1,25(OH)_2D_3$ restores hPDLSC osteogenesis dependently through the NRF2/HO-1 pathway.

## 4. Discussion

Diabetic periodontitis presents a significant clinical challenge due to the sustained high glucose microenvironment, which induces severe oxidative stress, impairs the regenerative potential of periodontal stem cells, and ultimately exacerbates alveolar bone loss. Conventional mechanical debridement often fails to predictably reconstruct the lost bone in these patients, necessitating the exploration of novel adjunctive therapies. This study systematically investigated the protective effects of $1,25(OH)_2D_3$ against high glucose-induced impairment in human periodontal ligament stem cells. Our findings demonstrate that $1,25(OH)_2D_3$ effectively mitigates oxidative stress, restores cell proliferation and migration, and reactivates the osteogenic differentiation program. Crucially, we elucidate that these therapeutic effects are mechanistically dependent on the targeted activation of the NRF2/HO-1 signaling pathway.

The cytocompatibility and biological effects of $1,25(OH)_2D_3$ are highly dose- and time-dependent. Consistent with previous reports, continuous high glucose exposure (25 mM) significantly suppressed hPDLSC proliferation and migration, mimicking the pathological microenvironment of severe diabetic periodontitis (Gao et al. 2025; Pham and Van Pham 2019). Interestingly, while short-term treatment with $1,25(OH)_2D_3$ robustly promoted cell viability, prolonged exposure to high concentrations paradoxically inhibited proliferation. This observation is not merely indicative of cytotoxicity, but rather aligns with the biological paradigm that mesenchymal stem cells must withdraw from the active cell cycle to initiate lineage-specific terminal differentiation (Wang et al. 2022; Chen et al. 2022). Consequently, establishing 100 nM at 24 h as the optimal intervention window allowed us to effectively halt the high glucose-induced acute damage while successfully transitioning the metabolic state of

hPDLSCs towards osteogenic differentiation.

At the core of high glucose-mediated cellular dysfunction lies the disruption of redox homeostasis. The excessive accumulation of reactive oxygen species overwhelms the endogenous antioxidant defense systems, triggering lipid peroxidation (MDA elevation) and extensive oxidative DNA damage (8-OHdG accumulation) (Yaribeygi et al. 2019; Tang et al. 2022; Ayala et al. 2014). In this study, we observed that high glucose severely compromised the basal expression of NRF2, the master regulator of the antioxidant response, and its downstream effector HO-1, leading to a decompensated state of oxidative stress and amplified pro-inflammatory cytokine (TNF-α, IL-6) secretion (Xiang et al. 2022; Xi et al. 2022). However, intervention with $1,25(OH)_2D_3$ potently antagonized this metabolic toxicity. Morphological and molecular evidence revealed that $1,25(OH)_2D_3$ actively promoted the nuclear translocation of NRF2, thereby rescuing the transcription and translation of HO-1 and restoring SOD activity. This robust activation of the NRF2/HO-1 axis effectively scavenged excessive ROS, alleviated lipid and DNA oxidative damage, and curtailed the inflammatory response, highlighting the profound immunomodulatory and antioxidant properties of $1,25(OH)_2D_3$.

The restoration of redox homeostasis by $1,25(OH)_2D_3$ serves as a prerequisite for the functional rescue of osteogenic potential. The high glucose-induced oxidative stress severely disrupts multiple osteogenic regulatory networks, leading to the downregulation of essential transcription factors (RUNX2, β-catenin) and phenotypic markers (ALP, OCN) (Tan et al. 2022; Huang et al. 2024; Komori 2022). We observed that $1,25(OH)_2D_3$ effectively antagonized this inhibition, orchestrating the re-expression and correct subcellular localization of RUNX2 (nuclear) and ALP (extranuclear), which ultimately culminated in restored extracellular matrix mineralization. To definitively confirm the mechanistic link, we employed the NRF2-specific inhibitor ML385. The targeted blockade of NRF2 nuclear translocation completely abolished the $1,25(OH)_2D_3$ mediated rescue of both the antioxidant defense (HO-1) and the osteogenic cascade (RUNX2, ALP, OCN). These reversal experiments compellingly demonstrate that the pro-osteogenic efficacy of $1,25(OH)_2D_3$ under high glucose conditions is strictly dependent on the activation of the NRF2/HO-1 signaling pathway (Han et al. 2022; Liu et al. 2023).

In conclusion, this study reveals that $1,25(OH)_2D_3$ actively reshapes the intracellular redox environment and reinitiates osteogenesis in hPDLSCs under high glucose stress

via the NRF2/HO-1 axis. These findings provide a solid theoretical basis for utilizing $1,25(OH)_2D_3$ as a promising targeted adjunctive therapy to overcome the bone regeneration obstacles commonly encountered in diabetic periodontitis.

## 5. Conclusion

In summary, high glucose induces severe oxidative stress and inflammation in hPDLSCs, impairing their osteogenic capacity. $1,25(OH)_2D_3$ treatment effectively reverses these impairments, restoring cell proliferation, migration, and differentiation. Mechanistically, these protective effects depend on activating the NRF2/HO-1 pathway to scavenge oxidative damage. These findings position $1,25(OH)_2D_3$ as a promising therapeutic strategy for diabetic alveolar bone regeneration.

## 6. Abbreviations

CCK-8: Cell counting kit-8

RT-qPCR: Real-time quantitative reverse transcription polymerase chain reaction

HG: High glucose

hPDLSCs: Human periodontal ligament stem cells

$1,25(OH)_2D_3$: 1,25-Dihydroxyvitamin $D_3$

GAPDH: Glyceraldehyde-3-phosphate dehydrogenase

FBS: Fetal bovine serum

PBS: Phosphate buffered saline

ROS: Reactive oxygen species

MDA: Malondialdehyde

SOD: Superoxide dismutase

8-OHdG: 8-Hydroxy-2'-deoxyguanosine

## References

Alves T, Alvarez-Rivas C, Mahatumarat N, Kantarci A (2026) Inflammation dynamics modulate periodontal stem cell fate and function. Frontiers in Immunology 17: 1783891

Ayala A, Muñoz MF, Argüelles S (2014) Lipid peroxidation: production, metabolism, and signaling mechanisms of malondialdehyde and 4-hydroxy-2-nonenal. Oxidative Medicine and Cellular Longevity 2014: 360438

Blufstein A, Behm C, Kubin B, Gahn J, Rausch-Fan X, Moritz A, Andrukhov O (2021) Effect of vitamin $D_3$ on the osteogenic differentiation of human periodontal ligament stromal cells under inflammatory conditions. Journal of Periodontal Research 56(3): 579-588

Borojević A, Jauković A, Kukolj T, Mojsilović S, Obradović H, Trivanović D, Živanović M, Zečević Ž, Simić M, Gobeljić B, Vujić D, Bugarski D (2022) Vitamin $D_3$ stimulates proliferation capacity, expression of pluripotency markers, and osteogenesis of human bone marrow mesenchymal stromal/stem cells, partly through sirt1 signaling. Biomolecules 12(2): 323

Cao L, Wang J (2026) Roles of Wnt/β-catenin signaling in osteoporosis, disease pathogenesis, and natural compound intervention. Biomolecules & Therapeutics 34(1): 65-79

Ceriello A, Prattichizzo F (2021) Variability of risk factors and diabetes complications. Cardiovascular Diabetology 20(1): 101

Chen C, Wan X, Shang J, Zhang W, Xie Z (2022) A review on the effects of vitamin D attenuating ischemia reperfusion injuries. International Journal of Food Properties 25(1): 522-40

Chen J, Bai Y, Ding Y, Wang L, Zhang W, Yang F (2025) Recent advances in metal-organic frameworks for therapeutic applications in periodontitis. Frontiers in Medicine 12: 1706849

Chen J, Hu C, Lu X, Yang X, Zhu M, Ma X, Yang Y (2024) ALDH2 alleviates inflammation and facilitates osteogenic differentiation of periodontal ligament stem cells in periodontitis by blocking ferroptosis via activating Nrf2. Functional & Integrative Genomics 24(5): 184

Chen Y, Ma X, Mai H, Lai P, Huang R, Alimujiang A (2025) The application of dental mesenchymal stem cells (DMSCs) in the repair of oral and maxillofacial defects. Frontiers in Bioengineering and Biotechnology 13: 1677422

Cheng Y, Liu P, Xiang Q, Liang J, Chen H, Zhang H, Yang L (2022) Glucagon-like peptide-1 attenuates diabetes-associated osteoporosis in ZDF rat, possibly through the RAGE pathway. BMC Musculoskeletal Disorders 23(1): 465

Gao S, Chen T, Deng C, Liu G, Wei Z (2025) An endoplasmic reticulum stress-responsive nanocomposite hydrogel for diabetic wound healing through a fibroblast-immune cell dual regulation hub. Journal of Nanobiotechnology 23(1): 689

Goltzman D (2018) Functions of vitamin D in bone. Histochemistry and Cell Biology 149(4): 305-312

Gong A, Liu Y, Xu F, Chu Y, Wu J, Goltzman D, Miao D (2022) Role of 1,25-dihydroxyvitamin D in alleviating alveolar bone loss and gingival inflammation in ligature-induced periodontitis. American Journal of Translational Research 14(5): 3079-3091

Hajishengallis G, Chavakis T, Lambris JD (2020) Current understanding of periodontal disease pathogenesis and targets for host-modulation therapy. Periodontology 2000 84(1): 14-34

Han J, Yang K, An J, Jiang N, Fu S, Tang X ( 2022) The role of NRF2 in bone metabolism—friend or foe? Frontiers in Endocrinology 13: 813057

He Y, Wang X, He Y, Zhao X, Lin J, Feng Y, Chen J, Luo F, Li Z, Li J, Tan H (2022) A bioinspired Janus polyurethane membrane for potential periodontal tissue

regeneration. Journal of Materials Chemistry B 2022 10(14): 2602-2616

Hu Y, Kuang Y, Li H, Li S, Wang H, Li H, Zeng D, Li J, Song J (2025) Low-intensity pulsed ultrasound alleviates periodontitis in mice with T2DM through Nrf2 pathway. APL Bioengineering 9(4): 046105

Huang Y, Wang J, Jiang C, Zheng M, Han M, Fang Q, Liu Y, Li R, Zhong L, Li Z (2024) ANXA2 promotes osteogenic differentiation and inhibits cellular senescence of periodontal ligament cells (PDLCs) in high glucose conditions. PeerJ 12: e18064

Komori T (2022) Whole aspect of Runx2 functions in skeletal development. International Journal of Molecular Sciences 23(10): 5776

Kwon T, Lamster IB, Levin L (2021) Current concepts in the management of periodontitis. International Dental Journal 71(6): 462-476

Li J, Cao Y, Xu J, Li J, Lv C, Gao Q, Zhang C, Jin C, Wang R, Jiao R, Zhu H (2023) Vitamin D improves cognitive impairment and alleviates ferroptosis via the Nrf2 signaling pathway in aging mice. International Journal of Molecular Sciences 24(20): 15315

Liu M, Chen R, Xu Y, Zheng J, Wang M, Wang P (2023) Exosomal miR-141-3p from PDLSCs alleviates high glucose-induced senescence of pdlscs by activating the Keap1-Nrf2 signaling pathway. Stem Cells International 2023: 7136819

Liu P, Cao B, Zhou Y, Zhang H, Wang C (2023) Human umbilical cord-derived mesenchymal stem cells alleviate oxidative stress-induced islet impairment via the Nrf2/HO-1 axis. Journal of Molecular Cell Biology 15(5): mjad035

Mateen MA, Alaagib N, Haider KH (2024) High glucose microenvironment and human mesenchymal stem cell behavior. World Journal of Stem Cells 16(3): 237-244

Meng L, Wen W (2025) Mitochondrial dysfunction in diabetic periodontitis: mechanisms and therapeutic potential. Journal of Inflammation Research 18: 115-126

Meng M, Xia Q, Li Y, Chen X, Wang Q, Chen J, Xu X, Wang H, Shu J, Lu J, Cheng L, Ye Z, Song B, Dong Q (2022) Enamel matrix derivative expedites osteogenic differentiation of BMSCs via Wnt/β-catenin pathway in high glucose microenvironment. Journal of Bone and Mineral Metabolism 40(3): 448-459

Norahan MH, Sivarasu S, Fayzullin A, Mbanefo C, Bikmulina P, Ashurko I, Khristidis I, Timashev P (2025) Bioengineering of periodontal tissues: cell therapy and biomaterials application. Bioengineering 12(11): 1213

Palacios C, Gonzalez L (2014) Is vitamin D deficiency a major global public health problem? The Journal of Steroid Biochemistry and Molecular Biology 144 Pt A: 138-145

Păunică I, Giurgiu M, Dumitriu AS, Păunică S, Pantea Stoian AM, Martu MA, Serafinceanu C (2023) The bidirectional relationship between periodontal disease and diabetes mellitus-a review. Diagnostics 13(4): 681

Pham HL, Van Pham P (2019) High glucose induces early senescence in adipose-derived stem cells by accelerating p16 and mTOR. Biomedical Research and Therapy 6(6): 3213-21

Plemmenos G, Piperi C (2022) Pathogenic molecular mechanisms in periodontitis and peri-implantitis: role of advanced glycation end products. Life 12(2): 218

Podembski, R., Barahona, I., Izidoro, C., Romero, A., & Mascarenhas, P (2025) Regenerative applications and performance of periodontal ligament stem cells: a comprehensive review of in vivo studies. Applied Sciences 15(21): 11444

Preshaw PM, Alba AL, Herrera D, Jepsen S, Konstantinidis A, Makrilakis K, Taylor R (2012) Periodontitis and diabetes: a two-way relationship. Diabetologia 55(1): 21-31

Song D, Chen B, Cheng T, Jin L, He J, Li Y, Liao C (2025) Attenuated NIX in impaired mitophagy contributes to exacerbating cellular senescence in experimental periodontitis

under hyperglycemic conditions. The FEBS Journal 292(7): 1726-1742

Tan J, Zhou Y, Luo J, Wu X, Liu H, Wang W, Li Z, Zhong M, Wu L, Li X (2022) High glucose inhibits the osteogenic differentiation of periodontal ligament stem cells in periodontitis by activating endoplasmic reticulum stress. Annals of Translational Medicine 10(4): 204

Tang L, Li T, Chang Y, Wang Z, Li Y, Wang F, Sui L (2022) Diabetic oxidative stress-induced telomere damage aggravates periodontal bone loss in periodontitis. Biochemical and Biophysical Research Communications 614: 22-28

Tian K, Xiong T, Zeng D, Huang Z, Liu R, Luo F (2025) Impact of reactive oxygen species on bone regeneration in diabetes: mechanisms and therapeutic strategies. Redox Biology 88: 103941

van Driel M, van Leeuwen JPTM (2023) Vitamin D and bone: a story of endocrine and auto/paracrine action in osteoblasts. Nutrients 15(3): 480

Wada S, Nakano H, Sawai Y, Yamauchi Y, Hasumoto M, Mitate E, Demura N (2026) Mechanistic and therapeutic insights into Nrf2-mediated redox regulation in periodontitis. Antioxidants 15(1): 72

Wang JW, Zhu L, Shi PZ, Wang PC, Dai Y, Wang YX, Lu XH, Cheng XF, Feng XM, Zhang L (2022) $1,25(OH)_2D_3$ mitigates oxidative stress-induced damage to nucleus pulposus-derived mesenchymal stem cells through PI3K/Akt pathway. Oxidative Medicine and Cellular Longevity 2022: 1427110

Wang M, Liu M, Zheng J, Xiong L, Wang P (2023) Exendin-4 regulates the MAPK and WNT signaling pathways to alleviate the osteogenic inhibition of periodontal ligament stem cells in a high glucose environment. Open Medicine 18(1): 20230692

Xi X, Li Z, Liu H, Chen S, Liu D (2022) Nrf2 activation is involved in cyclic mechanical stress-stimulated osteogenic differentiation in periodontal ligament stem cells via PI3K/Akt signaling and HO1-SOD2 interaction. Frontiers in Cell and

Developmental Biology 9: 816000

Xiang DD, Sun YX, Jiao C, Guo YQ, Fei YX, Ren BQ, He XT, Li X (2025) Diabetes and periodontitis: the role of a high-glucose microenvironment in periodontal tissue cells and corresponding therapeutic strategies. Stem Cell Research & Therapy 16(1): 366

Xiang Q, Zhao Y, Lin J, Jiang S, Li W (2022) The Nrf2 antioxidant defense system in intervertebral disc degeneration: molecular insights. Experimental & Molecular Medicine 54(8): 1067-1075

Yang Y, Li Q, Wei S, Chu K, Xue L, Liu J, Ma Y, Tao S (2022) STAT6/VDR axis mitigates lung inflammatory injury by promoting Nrf2 signaling pathway. Oxidative Medicine and Cellular Longevity 2022: 2485250

Yaribeygi H, Atkin SL, Sahebkar A (2019) A review of the molecular mechanisms of hyperglycemia-induced free radical generation leading to oxidative stress. Journal of Cellular Physiology 234(2): 1300-1312

Yuan L, Wang Y, Li N, Yang X, Sun X, Tian H, Zhang Y (2024) Mechanism of action and therapeutic implications of Nrf2/HO-1 in inflammatory bowel disease. Antioxidants 13(8): 1012

Zakaria MF, Sonoda S, Kato H, Ma L, Uehara N, Kyumoto-Nakamura Y, Sharifa MM, Yu L, Dai L, Yamauchi-Tomoda E, Aijima R, Yamaza H, Nishimura F, Yamaza T (2024) Erythropoietin receptor signal is crucial for periodontal ligament stem cell-based tissue reconstruction in periodontal disease. Scientific Reports 14(1): 6719

Zhang YL, Liu F, Li ZB, He XT, Li X, Wu RX, Sun HH, Ge SH, Chen FM, An Y (2022) Metformin combats high glucose-induced damage to the osteogenic differentiation of human periodontal ligament stem cells via inhibition of the NPR3-mediated MAPK pathway. Stem Cell Research & Therapy 13(1): 305

Zhang Z, Huang Q, Zhao D, Lian F, Li X, Qi W (2023) The impact of oxidative stress-

induced mitochondrial dysfunction on diabetic microvascular complications. Frontiers in Endocrinology 14: 1112363

Zhen L, Jiang X, Chen Y, Fan D (2017) MiR-31 is involved in the high glucose-suppressed osteogenic differentiation of human periodontal ligament stem cells by targeting Satb2. American Journal of Translational Research 9(5): 2384-2393

Zheng JX, Yin H, Tian GZ, Quan ZF, Dong ZL, Ding WQ, Wang ZX, Niu YT, Guo QY, Tang YQ, Guo WM (2025) Microenvironment-mediated stem cell fate in periodontal tissue remodeling and repair. Bioactive Materials 59: 69-95

## Figures captions

**Fig. 1** Isolation and characterization of hPDLSCs. (a) Primary cells migrating from tissue explants (b) Typical fibroblast-like morphology of passaged hPDLSCs. (c) Alizarin Red S staining after 21 days of osteogenic induction. (d) Oil Red O staining after 21 days of adipogenic induction. (e-h) Immunofluorescence staining of vimentin and cytokeratin. (i) Flow cytometric analysis of MSCs-specific surface markers.

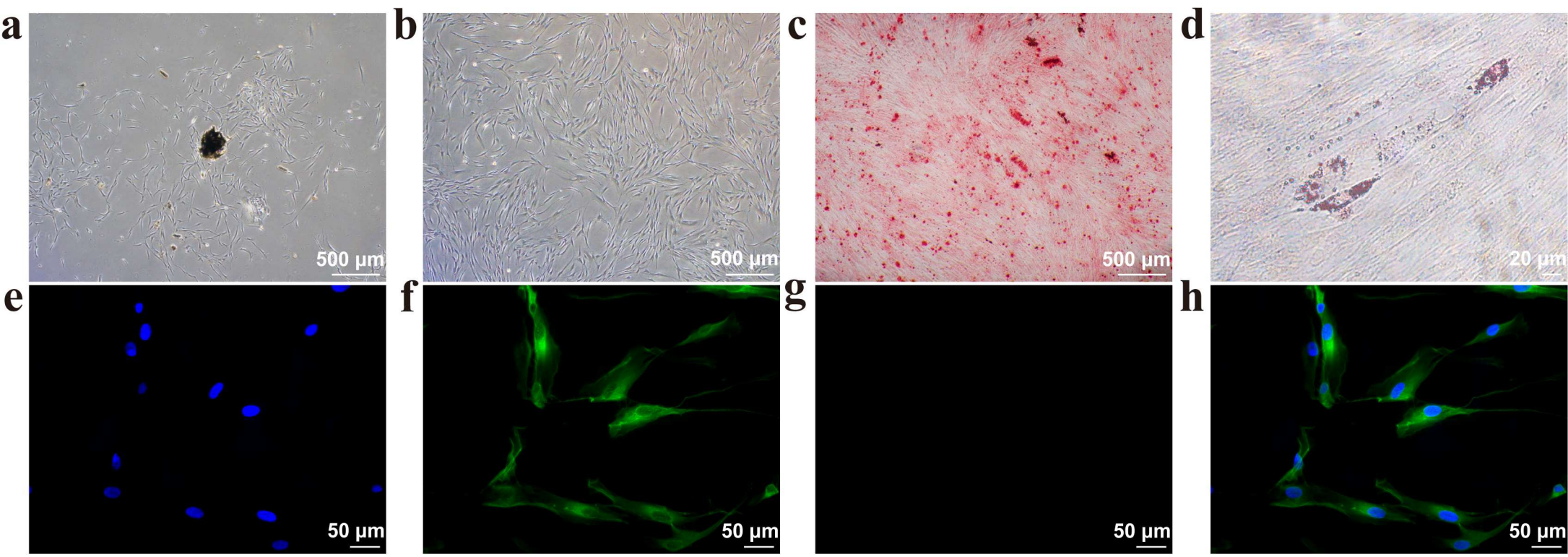
**Fig. 2** $1,25(OH)_2D_3$ alleviates high glucose-induced oxidative stress and restores proliferation and osteogenic differentiation in hPDLSCs (a) Cell proliferation of hPDLSCs treated with varying concentrations of $1,25(OH)_2D_3$ (1-300 nM) over time, evaluated by CCK-8 assay. (b) Cell viability of hPDLSCs cultured under varying glucose concentrations and a high mannitol (HM) osmotic control. (c) Dose- and time-dependent rescue effects of $1,25(OH)_2D_3$ (1, 10, and 100 nM) against high glucose-induced (25 mM) proliferative impairment. (d) Migration capacity of hPDLSCs evaluated by wound-healing assay under high glucose and $1,25(OH)_2D_3$ treatments over 24 h. (e) Intracellular ROS accumulation evaluated by flow cytometry and fluorescence microscopy. (f) Quantitative measurement of intracellular lipid peroxidation (MDA) levels. (g) Evaluation of endogenous superoxide dismutase (SOD) enzyme activity. (h) Alkaline phosphatase (ALP) staining and relative activity quantification after 7 days of osteogenic induction. (i) Alizarin Red S staining and quantitative analysis of extracellular matrix mineralization after 21 days of osteogenic induction.

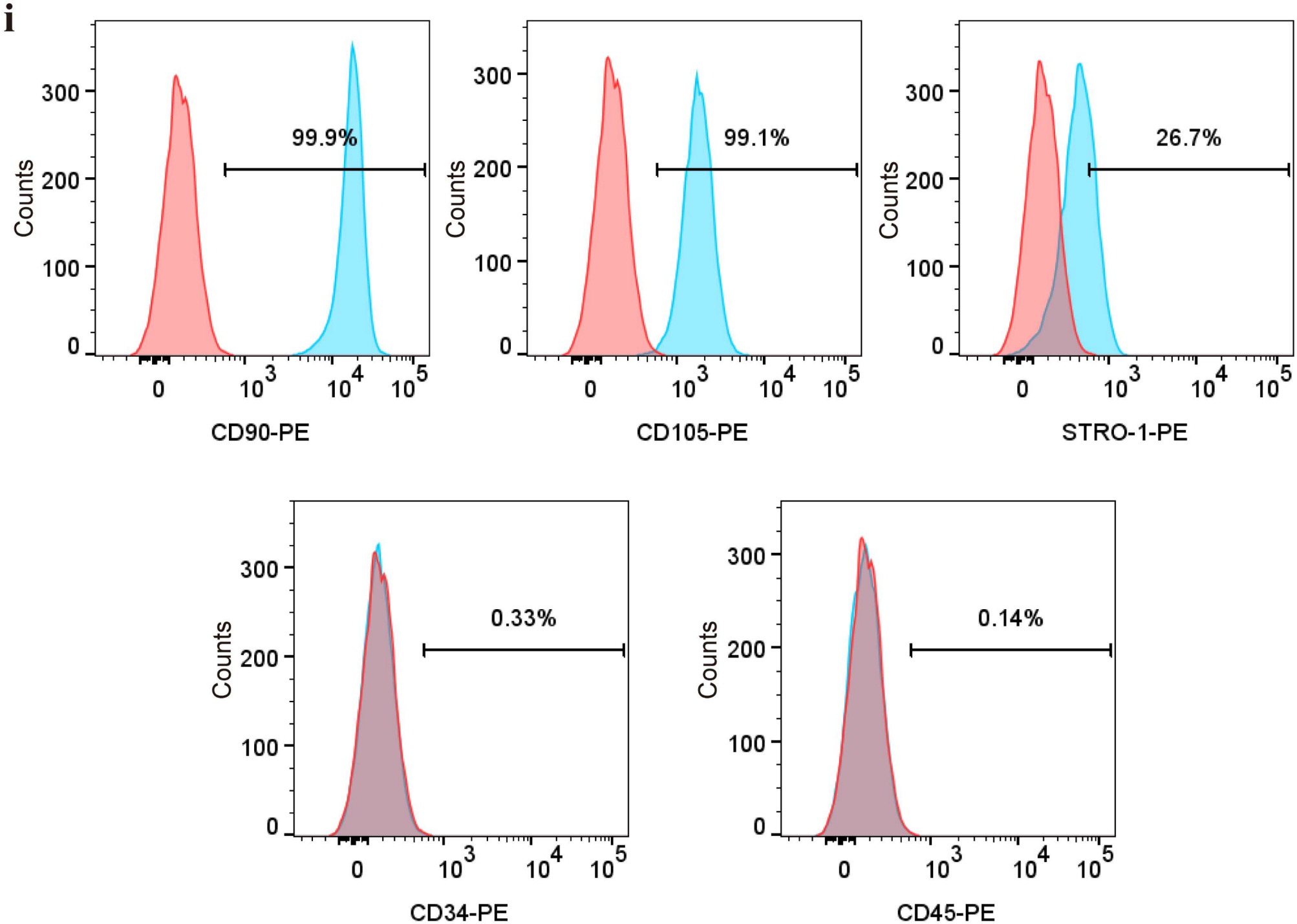
**Fig. 3** $1,25(OH)_2D_3$ mitigates high glucose-induced oxidative DNA damage and regulates the transcription, expression, and localization of antioxidant and inflammatory molecules (a) Relative mRNA expression levels of antioxidant (*NRF2*, *HO-1*) and pro-inflammatory (*TNF*-α, *IL-6*) genes evaluated by RT-qPCR. (b) Protein expression levels of the crucial antioxidant components NRF2 and HO-1 evaluated by Western blot. (c) Secretion levels of the pro-inflammatory cytokines TNF-α and IL-6 in culture supernatants, quantified by ELISA. (d) Immunofluorescence staining of intracellular 8-OHdG accumulation. (e, f) Immunofluorescence staining evaluating the expression and nuclear translocation of (e) NRF2, alongside the expression of (f) HO-1 in hPDLSCs.

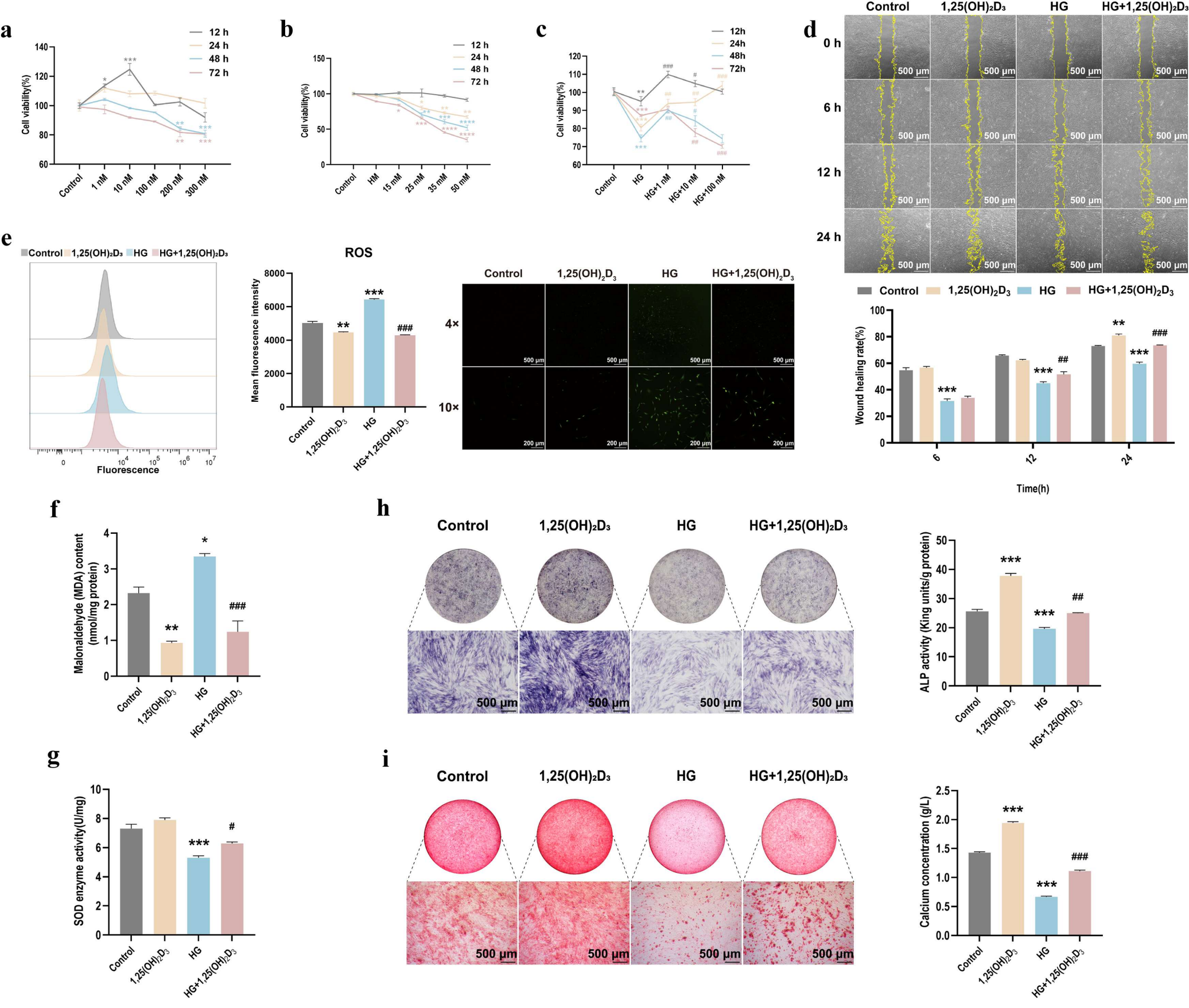
**Fig. 4** $1,25(OH)_2D_3$ restores the transcription, expression, and localization of osteogenic markers impaired by high glucose (a) Relative mRNA expression levels of core osteogenic markers (*ALP*, *RUNX2*, *OCN*, and β-*catenin*) after 7 days of induction, evaluated by RT-qPCR. (b) Protein expression profiles of ALP, RUNX2, OCN, and β-catenin evaluated by Western blot. (c, d) Immunofluorescence staining of ALP and RUNX2 in hPDLSCs after 7 days of osteogenic induction.

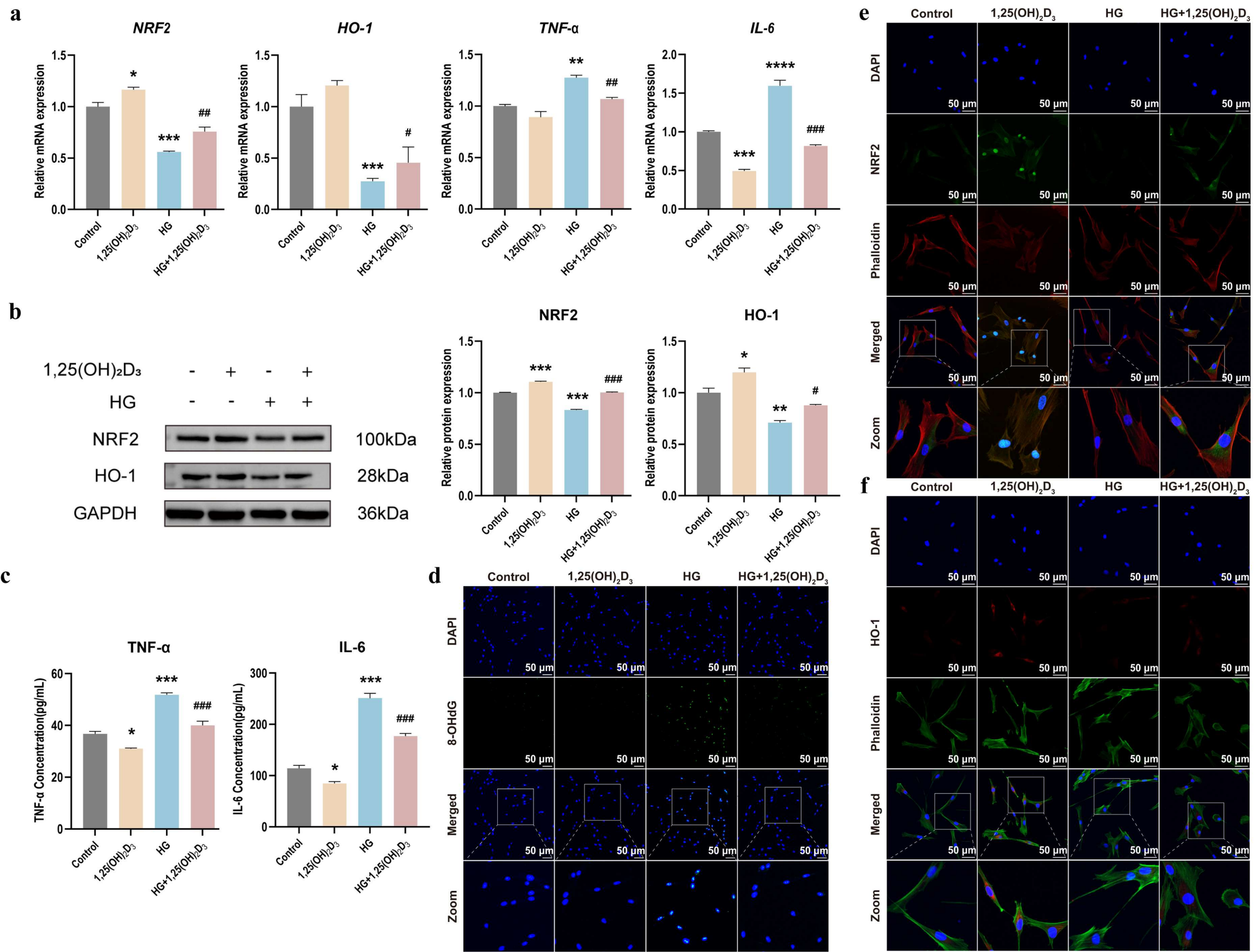
**Fig. 5** $1,25(OH)_2D_3$ activates the NRF2/HO-1 signaling pathway under high glucose conditions by promoting NRF2 nuclear translocation and HO-1 expression (a, b) Relative mRNA (a) and protein (b) expression levels of NRF2 and HO-1, evaluated with or without the NRF2 specific inhibitor ML385. (c, d) Immunofluorescence staining of (c) NRF2 and (d) HO1 in hPDLSCs treated with or without the NRF2 inhibitor ML385.

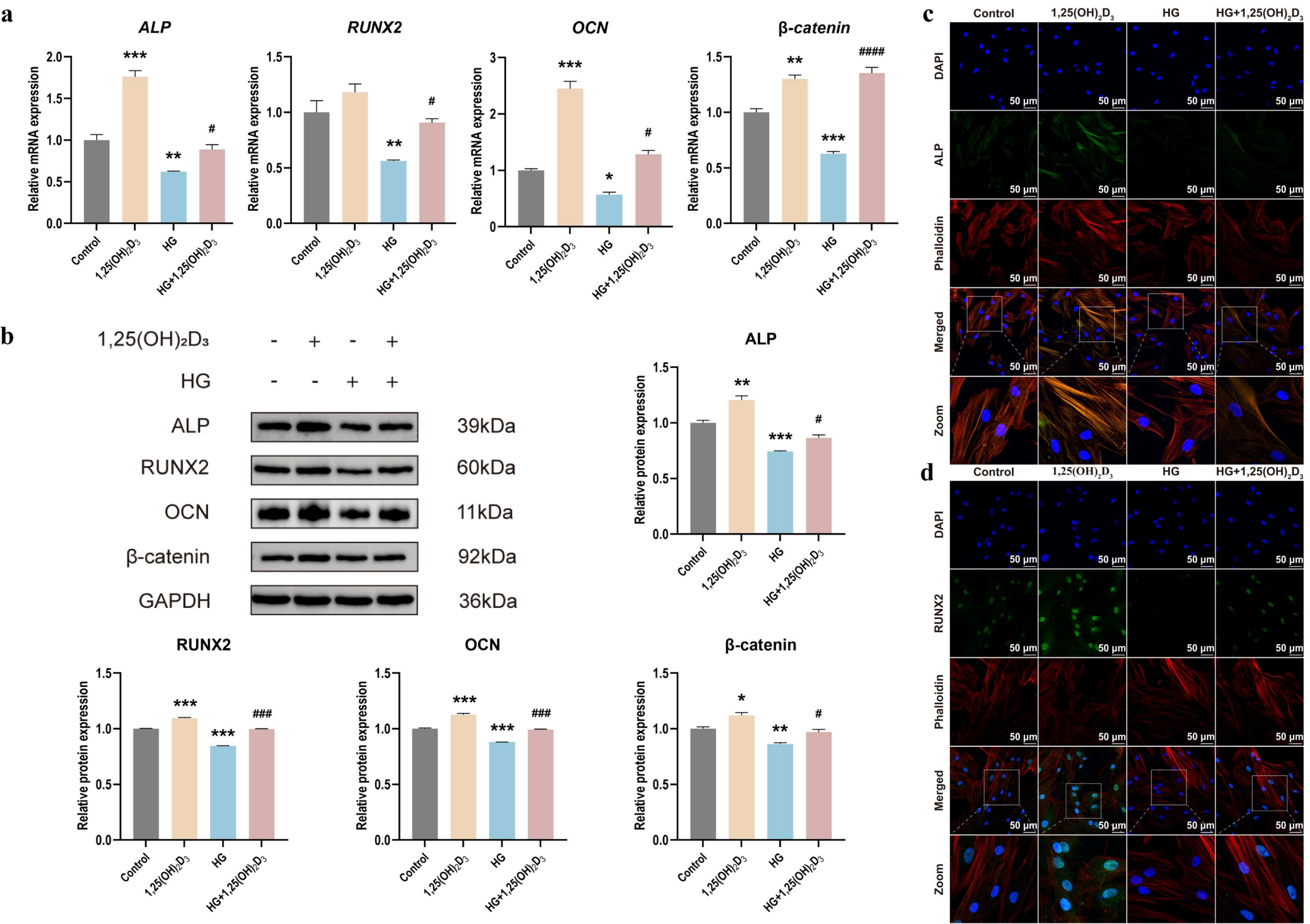
**Fig. 6** Inhibition of NRF2 attenuates the pro-osteogenic effects of $1,25(OH)_2D_3$ (a) ALP staining/activity and Alizarin Red S staining evaluating early and late osteogenic differentiation, respectively, with or without ML385. (b, c) Relative mRNA (b) and protein (c) expression profiles of core osteogenic markers (ALP, RUNX2, OCN, and β-catenin) evaluated with or without ML385.


a
500 μm
b
500 μm
c
500 μm
d
20 μm
e
50 μm
f
50 μm
g
50 μm
h
50 μm

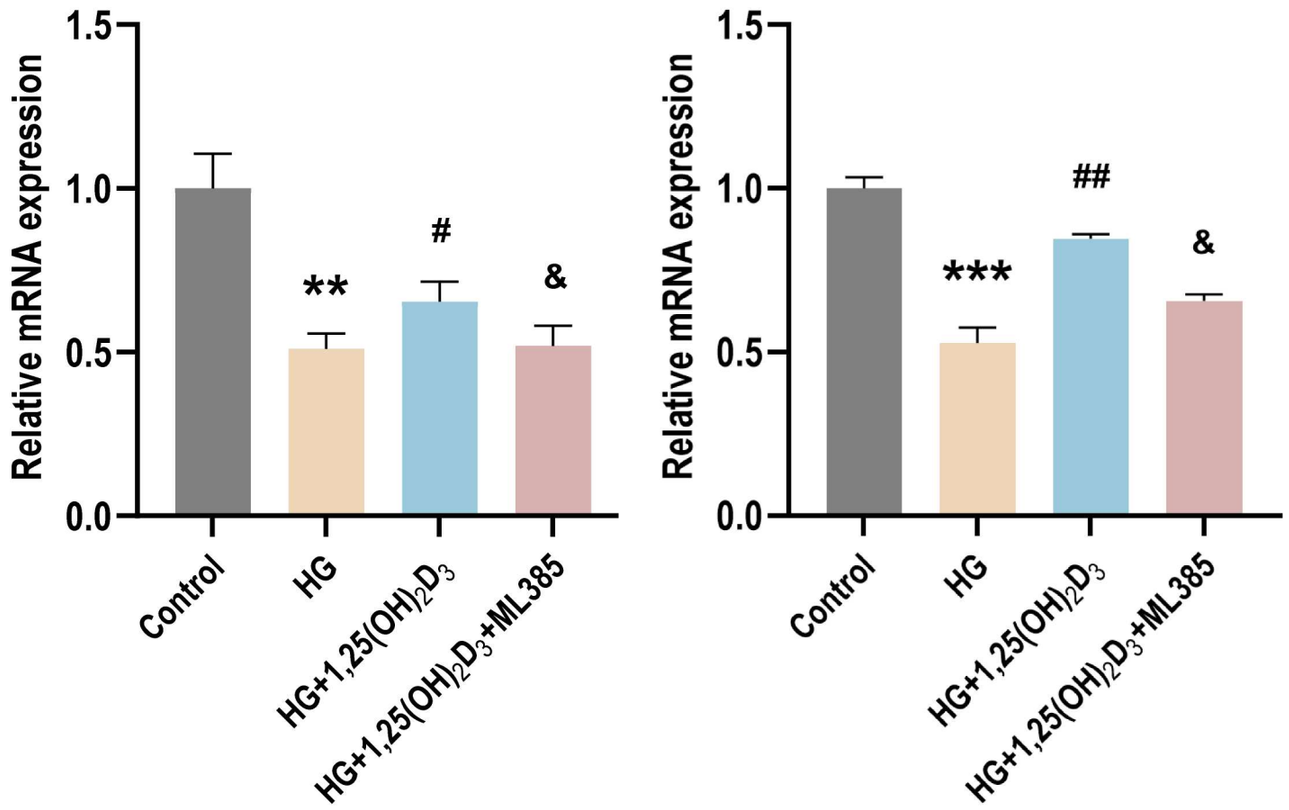

i
Counts
300
200
100
0
99.9%
0
10^3
10^4
10^5
CD90-PE
99.1%
CD105-PE
26.7%
STRO-1-PE
0.33%
CD34-PE
0.14%
CD45-PE


a
12 h
24 h
48 h
72 h
Cell viability(%)
Control
1 nM
10 nM
100 nM
200 nM
300 nM
b
12 h
24 h
48 h
72 h
Cell viability(%)
Control
HM
15 mM
25 mM
35 mM
50 mM
c
12h
24h
48h
72h
Cell viability(%)
Control
HG
HG+1 nM
HG+10 nM
HG+100 nM
d
Control
1,25(OH)₂D₃
HG
HG+1,25(OH)₂D₃
0 h
6 h
12 h
24 h
500 μm
Control
1,25(OH)₂D₃
HG
HG+1,25(OH)₂D₃
Wound healing rate(%)
Time(h)
e
Control
1,25(OH)₂D₃
HG
HG+1,25(OH)₂D₃
Fluorescence
ROS
Mean fluorescence intensity
Control
1,25(OH)₂D₃
HG
HG+1,25(OH)₂D₃
4×
10×
500 μm
200 μm
f
Malonaldehyde (MDA) content (nmol/mg protein)
Control
1,25(OH)₂D₃
HG
HG+1,25(OH)₂D₃
g
SOD enzyme activity(U/mg)
Control
1,25(OH)₂D₃
HG
HG+1,25(OH)₂D₃
h
Control
1,25(OH)₂D₃
HG
HG+1,25(OH)₂D₃
500 μm
ALP activity (King units/g protein)
Control
1,25(OH)₂D₃
HG
HG+1,25(OH)₂D₃
i
Control
1,25(OH)₂D₃
HG
HG+1,25(OH)₂D₃
500 μm
Calcium concentration (g/L)
Control
1,25(OH)₂D₃
HG
HG+1,25(OH)₂D₃

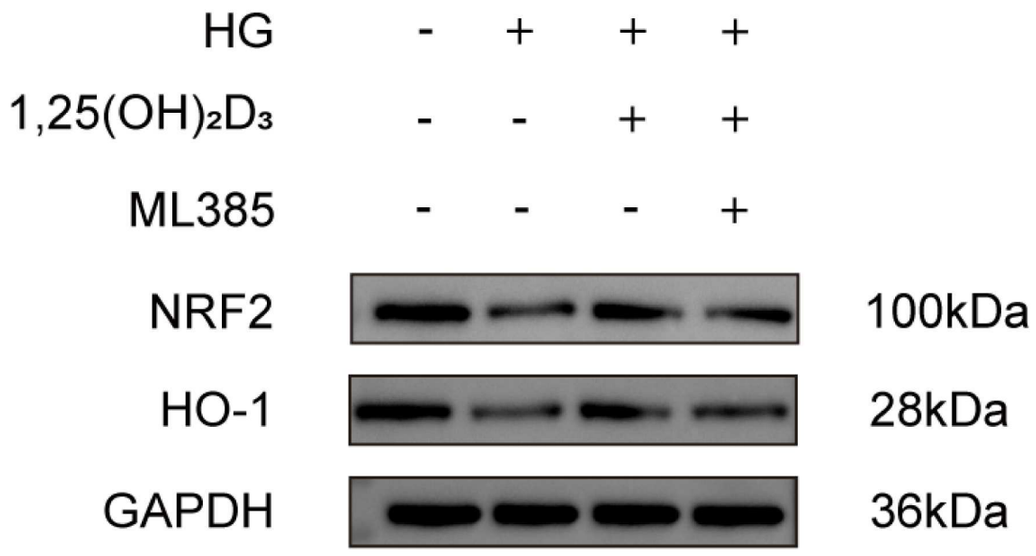

a
NRF2
HO-1
TNF-α
IL-6
Relative mRNA expression
Control
1,25(OH)2D3
HG
HG+1,25(OH)2D3
b
1,25(OH)₂D₃
HG
NRF2
HO-1
GAPDH
100kDa
28kDa
36kDa
Relative protein expression
c
TNF-α Concentration(pg/mL)
IL-6 Concentration(pg/mL)
d
DAPI
8-OHdG
Merged
Zoom
50 μm
e
f
HO-1
Phalloidin

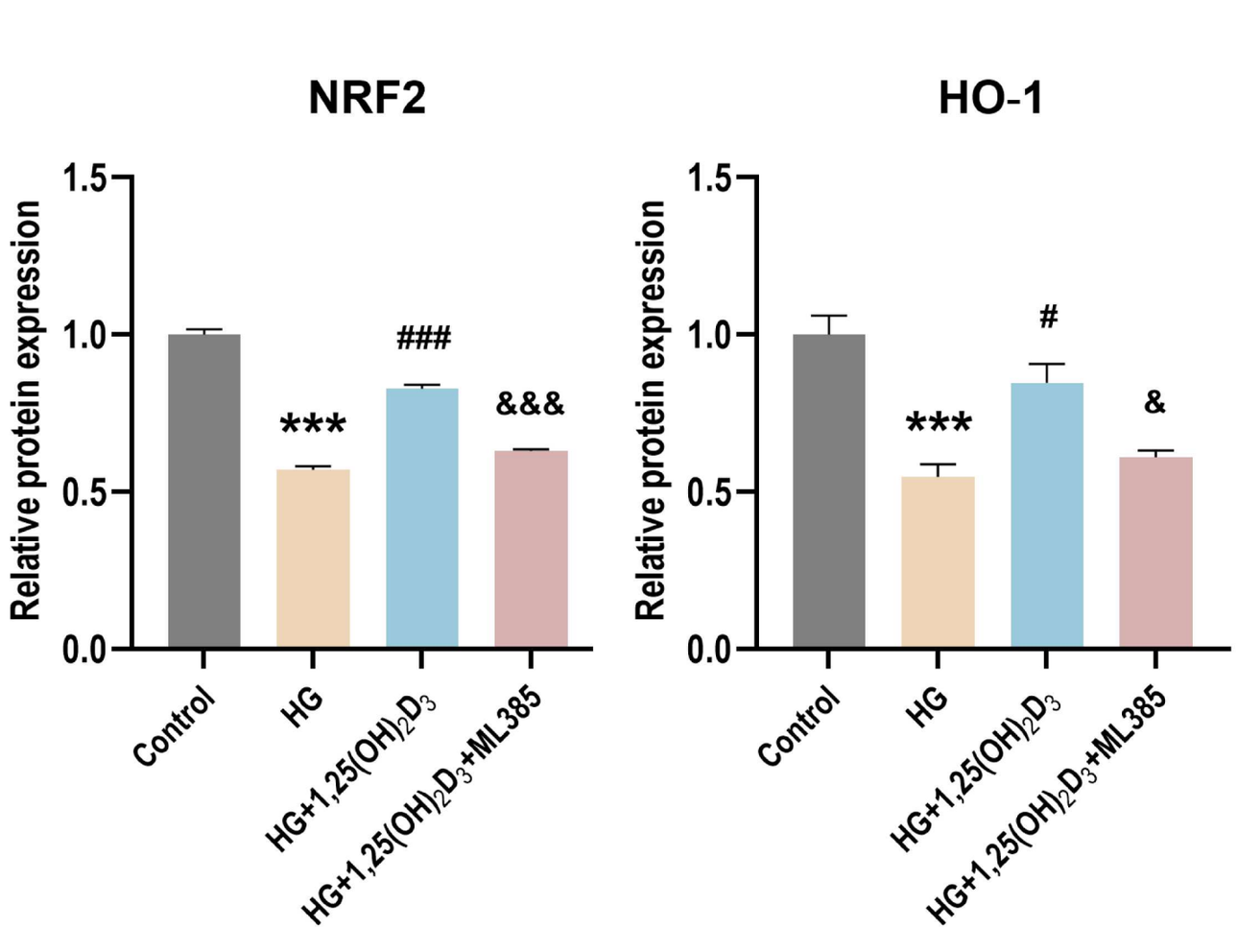

a
ALP
RUNX2
OCN
β-catenin
Relative mRNA expression
Control
1,25(OH)2D3
HG
HG+1,25(OH)2D3
b
1,25(OH)₂D₃
HG
ALP
RUNX2
OCN
β-catenin
GAPDH
39kDa
60kDa
11kDa
92kDa
36kDa
Relative protein expression
c
d
DAPI
Phalloidin
Merged
Zoom
50 μm

a

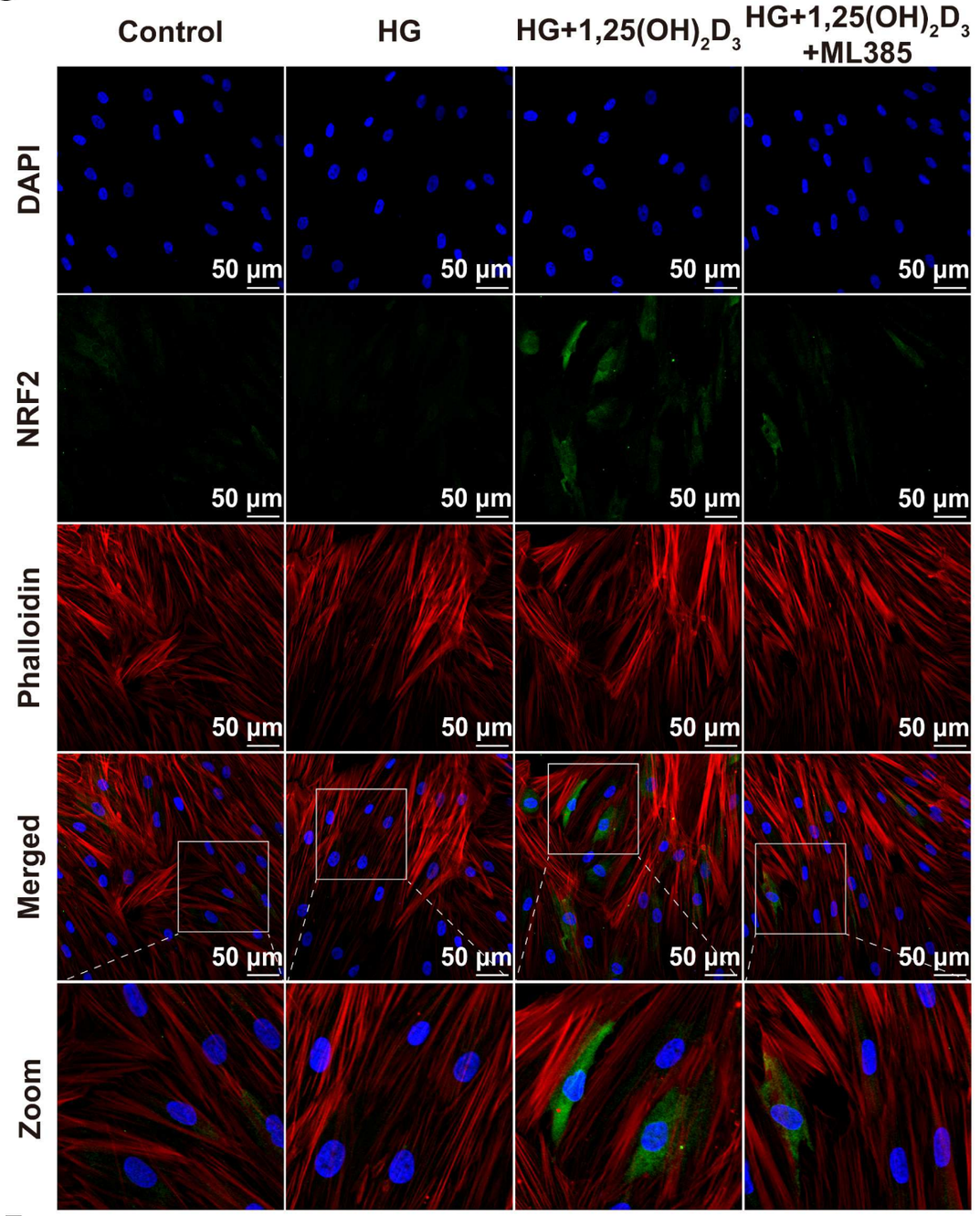

NRF2
Relative mRNA expression
1.5
1.0
0.5
0.0
**
#
&
Control
HG
HG+1,25(OH)2D3
HG+1,25(OH)2D3+ML385
HO-1
Relative mRNA expression
1.5
1.0
0.5
0.0
***
##
&
Control
HG
HG+1,25(OH)2D3
HG+1,25(OH)2D3+ML385

b

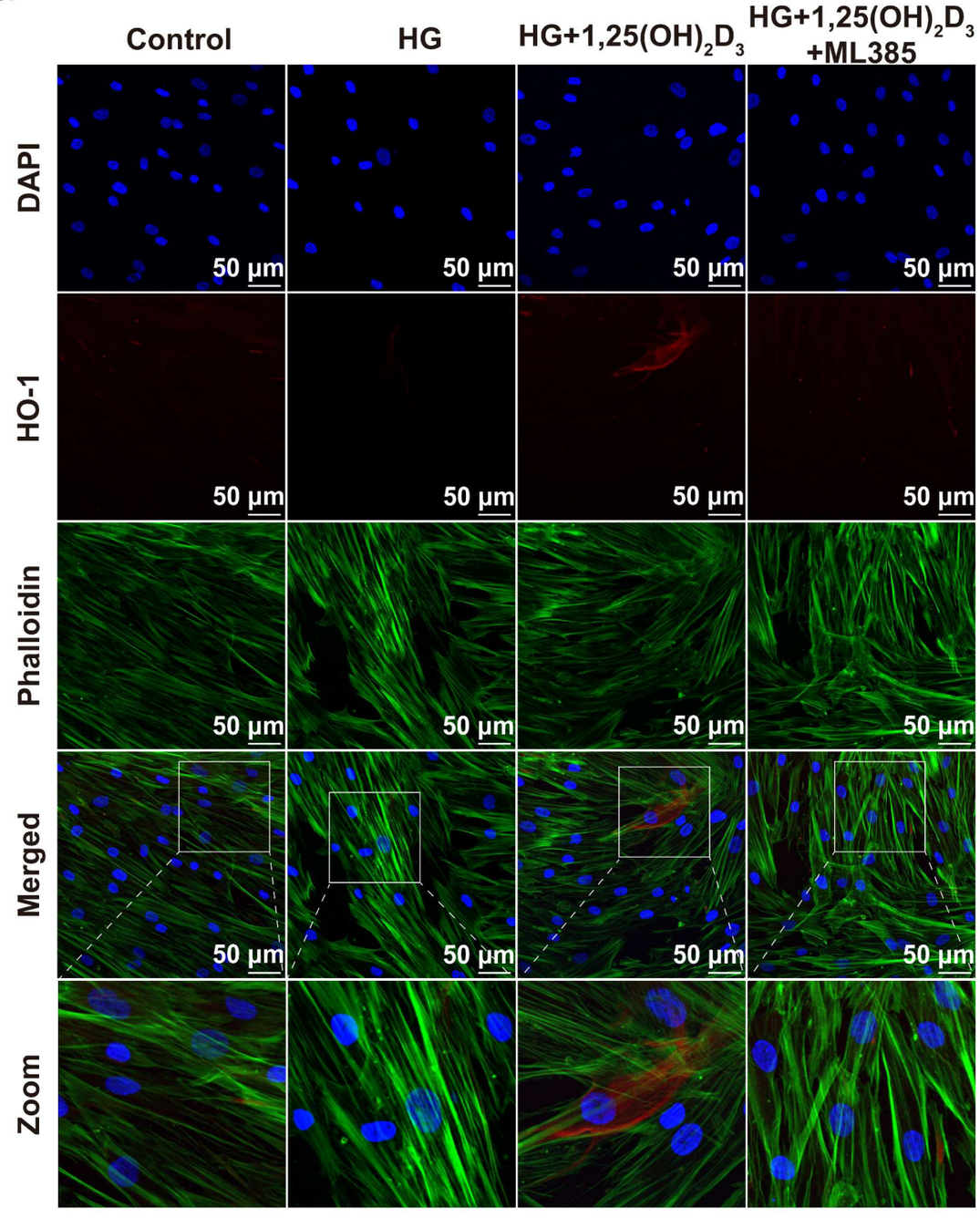

HG - + + +
1,25(OH)2D3 - - + +
ML385 - - - +
NRF2 100kDa
HO-1 28kDa
GAPDH 36kDa


NRF2
Relative protein expression
1.5
1.0
0.5
0.0
***
###
&&&
Control
HG
HG+1,25(OH)2D3
HG+1,25(OH)2D3+ML385
HO-1
Relative protein expression
1.5
1.0
0.5
0.0
***
#
&
Control
HG
HG+1,25(OH)2D3
HG+1,25(OH)2D3+ML385

c


Control
HG
HG+1,25(OH)2D3
HG+1,25(OH)2D3 +ML385
DAPI
NRF2
Phalloidin
Merged
Zoom
50 μm

d


Control
HG
HG+1,25(OH)2D3
HG+1,25(OH)2D3 +ML385
DAPI
HO-1
Phalloidin
Merged
Zoom
50 μm

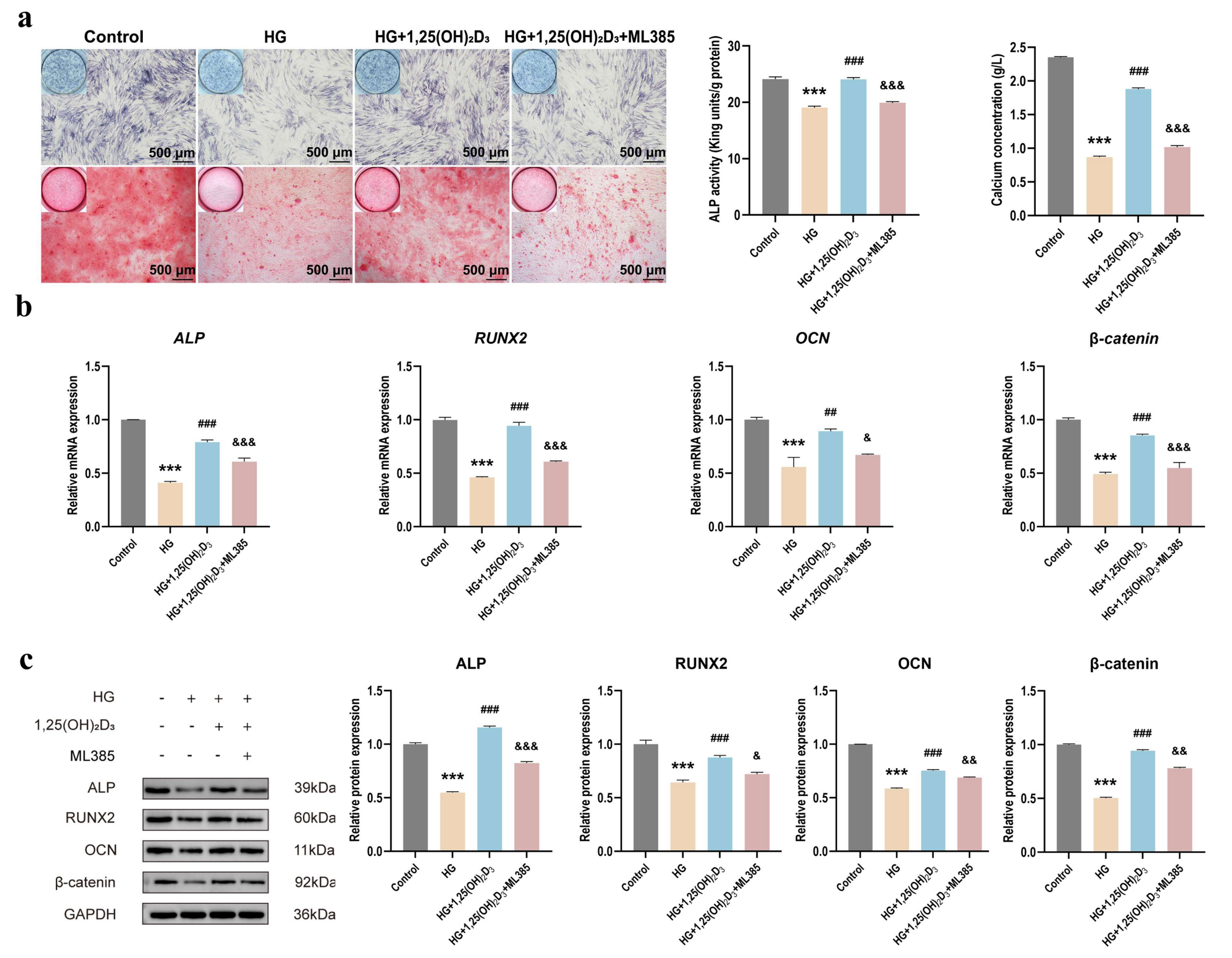

a
Control
HG
HG+1,25(OH)2D3
HG+1,25(OH)2D3+ML385
500 μm
ALP activity (King units/g protein)
Calcium concentration (g/L)
b
ALP
RUNX2
OCN
β-catenin
Relative mRNA expression
c
HG
1,25(OH)2D3
ML385
ALP
RUNX2
OCN
β-catenin
GAPDH
39kDa
60kDa
11kDa
92kDa
36kDa
Relative protein expression

Table 1. The primer sequences for analysed genes

| Target | Forward Primer Sequence (5′-3′) | Reverse Primer Sequence (5′-3′) |
|---|---|---|
| *NRF2* | TGCCAACTACTCCCAGGTTG | AACGTAGCCGAAGAAACCTCA |
| *HO-1* | TCTTGGCTGGCTTCCTTACC | GGATGTGCTTTTCGTTGGGG |
| *TNF*-α | CATCCAACCTTCCCAAACGC | CGAAGTGGTGGTCTTGTTGC |
| *IL-6* | CCACCGGGAACGAAAGAGAA | GAGAAGGCAACTGGACCGAA |
| *ALP* | AGGCTTGCCCCAAATCTCAA | GACCTTTGGCTCTCGACCAG |
| *RUNX2* | CACAAGTGCGGTGCAAACTT | TGACTCTGTTGGTCTCGGTG |
| *OCN* | CACCGAGACACCATGAGAGC | CTGCTTGGACACAAAGGCTG |
| β-*catenin* | TTTCCAGAAGCAGGAGTCCC | GGCTGTCAGGTTTGATCCCA |
| *GAPDH* | TGCAACCGGGAAGGAAATGA | GCATCACCCGGAGGAGAAAT |